© 2014. Published by The Company of Biologists Ltd | The Journal of Experimental Biology (2014) 217, 3815-3822 doi:10.1242/jeb.108985

RESEARCH ARTICLE

Allatostatin A-like immunoreactivity in the nervous system and gut of the larval midge *Chironomus riparius*: modulation of hindgut motility, rectal K^+ transport and implications for exposure to salinity

Lisa Robertson*, Helen Chasiotis*, Vladimir Galperin and Andrew Donini‡

ABSTRACT

Evidence for the presence of allatostatin (AST) A-like neuropeptides in the larval midge *Chironomus riparius* is reported. Immunohistochemical studies on the nervous system and gut revealed the presence of AST A-like immunoreactive (AST-IR) cells and processes. The nerve cord contained AST-IR processes that originated from cells in the brain and travelled the length of nerve cord to the terminal ganglion. Within each ganglion, these processes gave rise to varicosities, suggesting that they formed synapses with neurons in the ganglia. Endocrine cells containing AST-IR were present in three regions of the midgut: near the attachment of the Malpighian tubules, between the anterior and posterior midgut, and in the vicinity of the gastric caecae. The terminal ganglion also contained four AST-IR cells that gave rise to axons that projected onto the hindgut and posterior midgut. Application of a cockroach AST to the semi-isolated hindgut of larval *C. riparius* led to dose-dependent inhibition of muscle contractions with an EC_{50} of ~10 nmol l^{-1} and a decrease in rectal K^+ reabsorption resulting from reduced rectal Na^+/K^+-ATPase and vacuolar type H^+-ATPase activities. The results suggest the presence of endogenous AST-like neuropeptides in larval *C. riparius*, where these factors play a role in the function of the gut. Furthermore, regulation of ion reabsorption by ASTs at the rectum could serve as an ideal mechanism of ion regulation in the face of abrupt and acute elevated salt levels.

KEY WORDS: Na^+/K^+-ATPase, V-ATPase, Ion transport, Epithelium, Muscle, Ion regulation

INTRODUCTION

Juvenile hormones are synthesized by the corpora allata and control the juvenile characteristics of insects during growth and development. In adult insect females, juvenile hormones can also regulate reproductive activities such as the maturation of oocytes. Synthesis of juvenile hormones is inhibited by allatostatins (ASTs), members of a large and diverse family of peptides that are structurally characterized into three distinct groups (Gäde and Goldsworthy, 2003).

The C-type allatostatins with an N-terminal pGlu residue and a free C terminus have been discovered in the moth *Manduca sexta*, the fly *Drosophila melanogaster* and the mosquito *Aedes aegypti* (Kramer et al., 1991; Williamson et al., 2001; Li et al., 2006). The B-type allatostatins all have a common Trp-(X6)-Trp-amide C terminus and were first discovered in the cricket (Wang et al., 2004). The A-type allatostatins (ASTs) were the first to be discovered in the cockroach and share a Phe-Gly-Leu-amide C terminus (Donly et al., 1993; Siju et al., 2014).

All allatostatins inhibit juvenile hormone synthesis in at least one group or species of insect; however, many do not in other insects, and instead have known inhibitory activity on contractile properties of muscle (Gäde and Goldsworthy, 2003). In particular, the ASTs have been shown to inhibit contractions of visceral muscle including the foregut and hindgut (Lange et al., 1993; Sarkar et al., 2003; Predel et al., 2001; Matthews et al., 2008), and have been localized to endocrine cells of the gut (Veenstra et al., 1995; Veenstra, 2009; Reichwald et al., 1994; Robertson and Lange, 2010), suggesting that they may have a role in feeding and digestion. In the cockroach, ASTs have been shown to decrease food consumption (Aguilar et al., 2003). There is increasing evidence that ASTs modulate ion transport of various regions of the gut (Onken et al., 2004; Vanderveken and O'Donnell, 2014). An important group of insects in which ASTs have not been studied are the midges.

Midge (*Chironomus riparius* Meigen 1804) larvae are ubiquitous benthic inhabitants of freshwater lakes, ponds, marshes and rivers in temperate regions of the Northern Hemisphere and have become important bioindicators of environmental pollution resulting from industrial effluents, sewage effluents and other anthropogenic sources (Moreau et al., 2008; Faria et al., 2006). *Chironomus riparius* have also been observed in naturally occurring and anthropogenically induced salinated water (Colbo, 1996; Williams and Williams, 1998). Endocrine disruptors affect midge larvae by altering the accumulation of yolk protein in eggs, inducing expression of Hsp70, activating the enzymes catalase and glutathione-S-transferase, and reducing the rate of successful adult emergence (Lee and Choi, 2007; Morales et al., 2011; Hahn et al., 2002). Despite their importance, very little is known about the physiological mechanisms that underlie the observed responses to xenobiotics, heavy metals, endocrine disruptors and salinity in midge larvae. In particular, to the best of our knowledge, there is only a single study that has examined neuroendocrine factors in midge larvae, revealing the presence of serotonin and the peptides proctolin and bombesin in neurons of *Chironomus tentans* (Johansson et al., 1986).

Because allatostatins play a role in development and control aspects of feeding and digestion, factors that are affected by pollutants and endocrine disruptors in midges, it was hypothesized that allatostatins are present in midge larvae, where they could affect gut motility and ion transport. This study examined the presence of

Department of Biology, York University, 4700 Keele Street, Toronto, ON, M3J 1P3, Canada.
*Joint first authors

‡Author for correspondence (adonini@yorku.ca)

Received 1 June 2014; Accepted 2 September 2014

The Journal of Experimental Biology (2014) doi:10.1242/jeb.108985

List of abbreviations

AST	allatostatin
AST-IR	allatostatin-A (family of peptides with C-terminal ending of FGLamide) immunoreactivity
CNS	central nervous system
Dippu-AST7	peptide with APSGAQRLYGFGLamide sequence isolated from the cockroach *Diploptera punctata*
ISME	ion-selective microelectrode
NKA	Na^+/K^+-ATPase from the P-type family of ATPases
NSS	normal sheep serum
PBS	phosphate-buffered saline
SIET	scanning ion-selective electrode technique
VA	vacuolar-type H^+-ATPase

AST-like immunoreactivity (AST-IR) in the nervous system and the gut of the larval midge *C. riparius*. A novel midge larval hindgut motility assay was developed to assess potential effects of ASTs on the hindgut musculature. Effects of ASTs on rectal ion transport and rectal Na^+/K^+-ATPase (NKA) and vacuolar-type H^+-ATPase (VA) activities were also determined. The results led to an unexpected link between the effects of ASTs in midge larvae and larval habitat salinity.

RESULTS

AST-IR in the gut and nervous system

AST-IR is present throughout the ventral nerve cord and gut of larval *C. riparius* (Fig. 1). Diagrammatical representations of AST-IR in neurons, neural processes and neuroendocrine cells in the gut and nervous system are shown in Fig. 2. The midgut contains three regions with AST-IR endocrine-like cells (Fig. 1A,B, Fig. 2A). One region is located at the middle midgut (Fig. 1A, Fig. 2A), another region is located at the posterior midgut near the attachment of the Malpighian tubules (Fig. 1B, Fig. 2A), and some endocrine-like cells were found in the vicinity of the gastric caecae, albeit in fewer numbers with respect to the other two regions (Fig. 2A). The endocrine-like cells possessed a single short process that extended from the soma towards the midgut lumen (Fig. 1A, inset).

A number of AST-IR cells are located in the brain and give rise to neuropile and processes that run posteriorly into the nerve cord (Fig. 1C, Fig. 2B). These processes extend the length of the abdominal nerve cord through the connectives between ganglia and within the ganglia (Fig. 2B). As the processes pass through the ganglia, they have varicosities along their length (Fig. 1D). No AST-IR cell bodies are found in the abdominal ganglia; however, the terminal ganglion contains four AST-IR cells (Fig. 1E, Fig. 2B) and at least two of these give rise to processes in the proctodeal nerves, which innervate the rectum, ileum and posterior midgut (Fig. 1B,F–H, Fig. 2). The AST-IR in these is not continuous and instead appear as distinct punctate varicosities along the process (see Fig. 1B,G,H). Controls where the primary AST antiserum was omitted or pre-absorbed with 10^{-5} mol l^{-1} *Diploptera puncata* allatostatin 7 (Dippu-AST7) resulted in no staining throughout the gut and nervous system (data not shown).

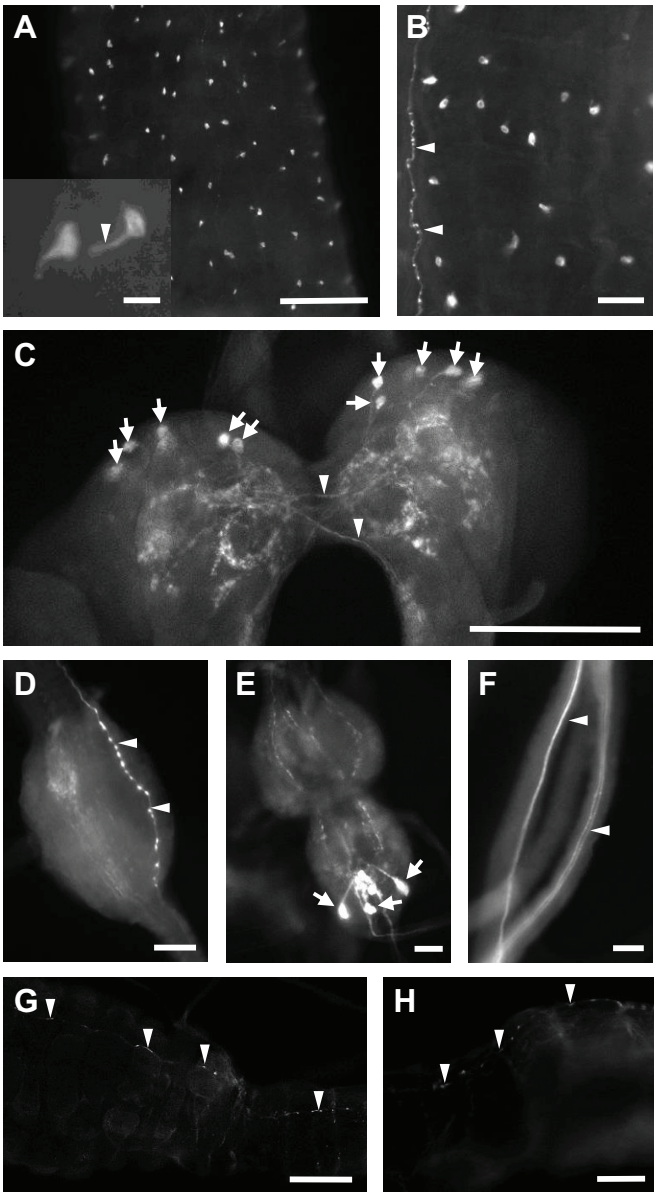

Fig. 1. Allatostatin-like immunoreactivity (AST-IR) in the central nervous system and gut of larval *Chironomus riparius*. (A) Anterior midgut with AST-IR endocrine cells. Inset: two AST-IR endocrine cells. (B) Posterior midgut with AST-IR endocrine cells. Arrowheads point to an AST-IR process originating from cells in the terminal ganglion. Inset arrowhead points to a process from an endocrine cell. (C) Brain. Arrows point to AST-IR neurons; arrowheads point to processes crossing the midline. (D) Representative abdominal ganglion. Arrowheads point to a process with varicosities. (E) Terminal ganglion. Arrows indicate soma of AST-IR cells. (F) Proctodeal nerves from the terminal ganglion that innervate the hindgut. Arrowheads point to AST-IR processes. (G) Portion of rectum and ileum with AST-IR process (arrowheads). (H) Portion of rectum with AST-IR process (arrowheads). Scale bars: (A) 100 µm, inset 10 µm; (B) 20 µm; (C) 100 µm; (D) 20 µm; (E) 20 µm; (F) 10 µm; (G) 100 µm; (H) 50 µm.

Effects of Dippu-AST7 on hindgut contractions

The semi-isolated larval hindgut of *C. riparius* bathed in a physiological saline contracted in a non-rhythmic manner and these contractions can be detected with an impedance monitor and viewed with data acquisition software. Each single contraction produced a vertical deflection of the recording voltage trace that was easily discernible above background noise (Fig. 3). It was not possible to localize contractions to specific regions of the hindgut because contractions of the ileum or rectum were detected by the impedance electrodes. Contractions that were visibly seen to occur at the posterior midgut were not detected by the impedance electrodes because the minutin pins inserted at the posterior midgut limited movements of this region.

In the presence of Dippu-AST7, the frequency of hindgut contractions decreased with respect to the frequency of

The Journal of Experimental Biology (2014) doi:10.1242/jeb.108985

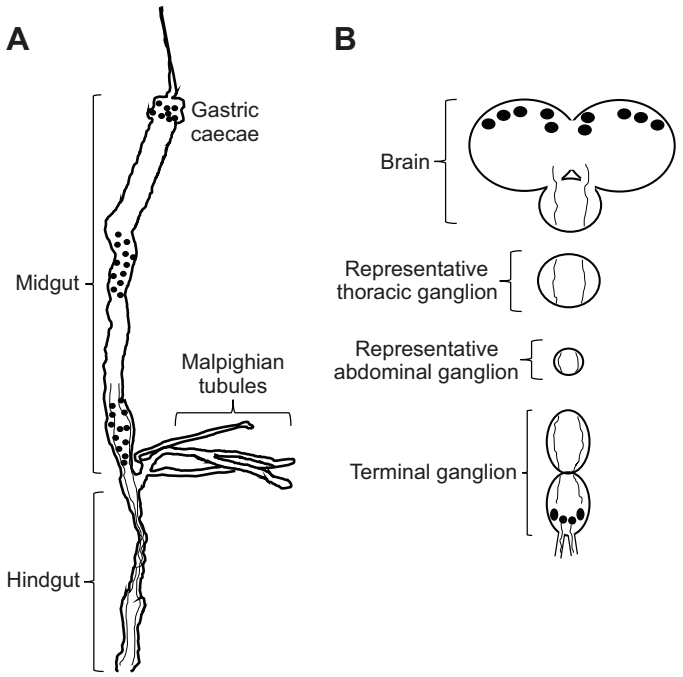

Fig. 2. Diagrammatical representation of AST-IR in the central nervous system and gut of larval *C. riparius*. (A) Gastrointestinal tract. Black circles represent AST-IR neuroendocrine cells. Three distinct regions of AST-IR neuroendocrine cells are located in the midgut. AST-IR processes on the hindgut and lower midgut, originating from neurons in the terminal ganglion, are shown. (B) Brain, representative thoracic and abdominal ganglia, and terminal ganglion. Black circles represent AST-IR neurons. AST-IR processes originating from the brain and extending the length of the nervous system are shown. Processes originating from a pair of neurons in the terminal ganglion which project to the hindgut are shown. Diagrams are not to scale.

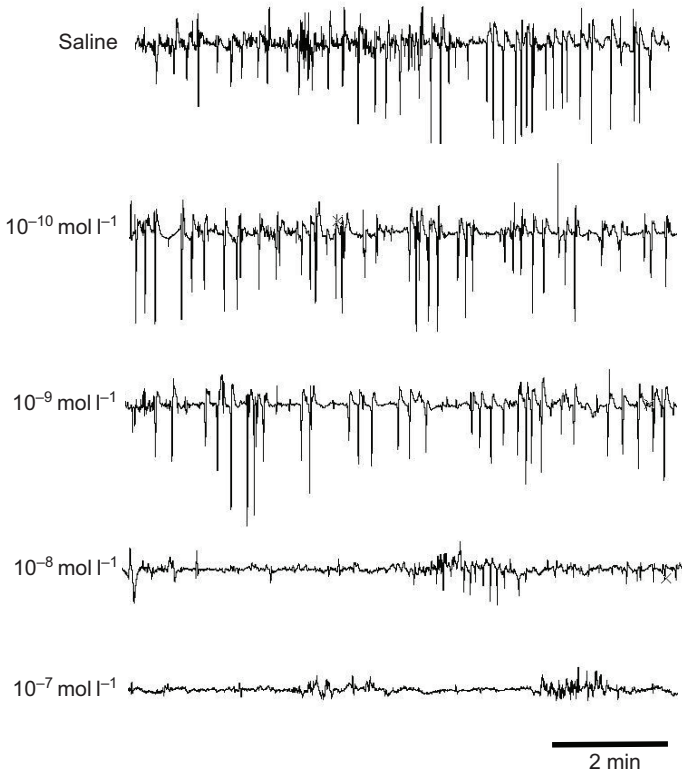

Fig. 3. Hindgut muscle contractions of larval *C. riparius*. Contractions were detected and recorded with an impedance monitor connected to a data acquisition system. Contractions appear as vertical deflections on the traces and these were monitored in either saline (spontaneous) or the indicated dose of Dippu-AST7.

contractions recorded in physiological saline without the peptide (Fig. 3, compare saline with Dippu-AST7 doses). This effect was dependent on the dose of Dippu-AST7, where increasing doses resulted in fewer hindgut contractions. Dippu-AST7 inhibited hindgut contractions with a threshold dose of ~0.5 nmol l^{-1} and an EC_{50} of ~10 nmol l^{-1} (Fig. 4). Application of 1 µmol l^{-1} Dippu-AST7 did not abolish contractions but inhibited the contractions by ~95%.

Effects of Dippu-AST7 on K^+ absorption by the rectum, and NKA and VA activities in the rectum

The rectum of larval *C. riparius* is a site of K^+ absorption (see Jonusaite et al., 2013). The mean baseline K^+ flux (absorption, lumen to bath) measured at the recta in this study was 104.3±13.7 pmol cm^{-2} s^{-1} (n=38). Addition of various doses of Dippu-AST7 to the recta resulted in a dose-dependent decrease in the K^+ flux (Fig. 5). Addition of saline (control) or a low dose of Dippu-AST7 (1 pmol l^{-1}) did not affect the K^+ fluxes. The highest dose of Dippu-AST7 tested (1 µmol l^{-1}) resulted in K^+ fluxes that were roughly half of the initial baseline K^+ flux.

NKA and VA activities in the rectum of larval *C. riparius* were ~15 to 20 times higher than in other regions of the gut including the Malpighian tubules, and evidence was provided that NKA and VA drive K^+ absorption at the rectum (see Jonusaite et al., 2013). Incubation with 10 nmol l^{-1} Dippu-AST7 for 10 min decreased the NKA and VA activities of the rectum by approximately one-third and two-thirds, respectively (Fig. 6).

NKA and VA protein expression in recta of freshwater- and brackish-water-reared larvae

A previous study demonstrated that recta of brackish-water-reared larvae have lower activities of NKA and VA compared with recta of freshwater-reared larvae (Jonusaite et al., 2013). Therefore, salinity and AST7 have similar effects on rectal NKA and VA activities. The actions of AST7 occur rapidly and hence cannot be mediated by changes in NKA and VA expression; however, it was suggested that larvae reared in brackish water may have lower expression of rectal NKA and VA than those reared in freshwater (Jonusaite et al., 2013). In an effort to determine whether the mechanisms of AST7- and salinity-induced changes in NKA and VA rectal activities are similar or different, NKA and VA protein expression studies on freshwater- and brackish-water-reared larvae were carried out.

The NKA α subunit was detected by western blot as a single band at ~95 kDa in recta collected from *C. riparius* larvae (Fig. 7A). Recta from larvae reared in brackish water, however, exhibited approximately fourfold less NKA α subunit protein expression than recta collected from freshwater (control)-reared larvae (Fig. 7B). In all samples examined, the VA B subunit was detected as a single band at ~56 kDa by western blot; however, a second band at ~58 kDa was also occasionally detected, but this did not appear to be correlated with rearing salinity (Fig. 7A). Densitometric analysis of the ~56 kDa band revealed relatively variable VA B subunit protein expression within recta collected from the freshwater-reared group (Fig. 7B). VA B subunit protein expression within recta collected from freshwater-reared larvae was not significantly different from protein levels in recta from the brackish-water-reared group (Fig. 7B). Actin expression, which was used as a loading

The Journal of Experimental Biology (2014) doi:10.1242/jeb.108985

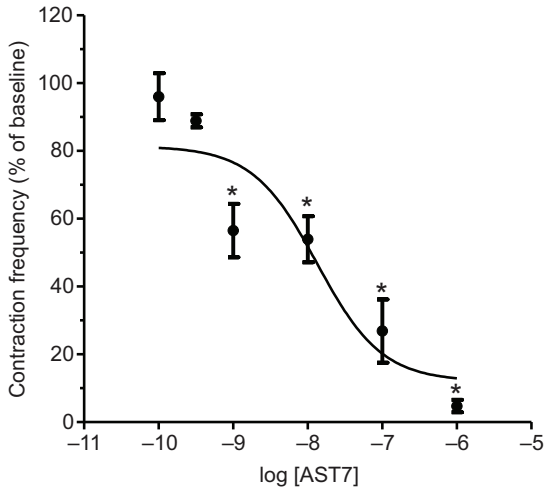

Fig. 4. Effect of Dippu-AST7 on the frequency of hindgut contractions. Contraction frequency measured in the presence of the peptide was expressed as the percentage of baseline frequency of contractions measured prior to the addition of the peptide. Data are plotted as means ± s.e.m. (n=4–14). Addition of saline without peptide was used as a control (not shown) and resulted in a mean of 105±7.2% of baseline frequency of contractions. Asterisks denote a significant difference from the control (ANOVA, P<0.001; Tukey–Kramer multiple comparisons test, P<0.05; non-linear curve fit R^2=0.8).

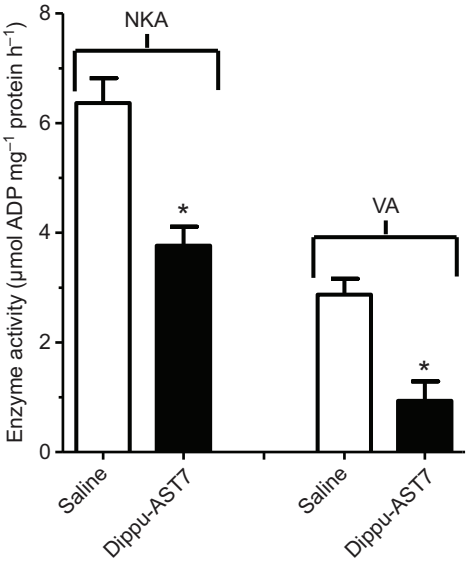

Fig. 6. Effects of 10^{-8} mol l^{-1} Dippu-AST7 on NKA and VA activities in the rectum of larval *C. riparius*. Isolated recta were incubated in either saline (control) or saline containing 10^{-8} mol l^{-1} Dippu-AST7 for 10 min. After incubation, the recta were flash-frozen and processed for NKA and VA activity assays. Asterisks denote a significant difference from the saline control (Student's t-test, P<0.05, n=5).

control to normalize NKA and VA protein abundance, was not significantly different (Student's t-test, P=0.4232; data not shown) between recta collected from control and brackish-water-reared larvae.

DISCUSSION

AST-like immunoreactivity in the nervous system and gut

Allatostatin immunoreactivity has been well documented in the nervous systems of insects with AST-IR cell bodies routinely found in the brain and abdominal ganglia (Skiebe et al., 2006; Žitňan et al., 1993; Kreissl et al., 1999; Lange et al., 1993; Hernández-Martínez et al., 2005). In *C. riparius* larvae, the brain contains at least five paired AST-IR cell bodies at the anterior edge of the frontal lobes (Fig. 1C, Fig. 2B). Processes originating from these cells appear to enter the central complex, which contains extensive AST-IR. Processes cross the center of the brain to the respective contralateral side and are seen running posteriorly into the nerve cord. In *C. riparius* larvae, only the terminal ganglion contained AST-IR cell bodies while only processes with many varicosities were present in the remaining ganglia (Fig. 1D,E, Fig. 2B). The processes in the ganglia are likely to originate from the neurons in the brain, suggesting that allatostatins act as neurotransmitters relaying information from the brain to other neurons in the ganglia of the ventral nerve cord in larval *C. riparius*. Similar processes have been found in other insects (Skiebe et al., 2006; Žitňan et al., 1993). At least one of the two pairs of lateral neurons in the terminal ganglion give rise to processes that innervate the hindgut (see Fig. 1F–H, Fig. 2B) and these processes extend the length of the rectum, ileum and onto the posterior midgut (Fig. 1B, Fig. 2A). Nerves containing AST-IR cell bodies on the hindgut that originate from neurons in the terminal ganglion/neuromere have been found in the cockroach, locust, moth, fruit fly and mosquito (Maestro et al., 1998; Yoon and Stay, 1995; Duve et al., 1997; Robertson and Lange, 2010; Hernández-Martínez et al., 2005). In the cockroach, branches of at least one pair of AST-like IR neurons project to the hindgut and were also seen to extend onto the midgut (Maestro et al., 1998). In the larval moth *Cydia pomonella*, larval *Drosophila* and adult mosquitoes, the processes from the terminal ganglion neurons are confined to the hindgut (Duve et al., 1997; Yoon and Stay, 1995; Hernández-Martínez et al., 2005).

In larval *C. riparius*, AST-IR endocrine cells are found in the posterior midgut near the attachment of the Malpighian tubules to the gut (Fig. 1B, Fig. 2A). Another group of endocrine cells is located in the middle midgut region (Fig. 1A, Fig. 2A) and a third group is found in the anterior midgut associated with the gastric caecae (Fig. 2A). Other dipteran species have regional groups of

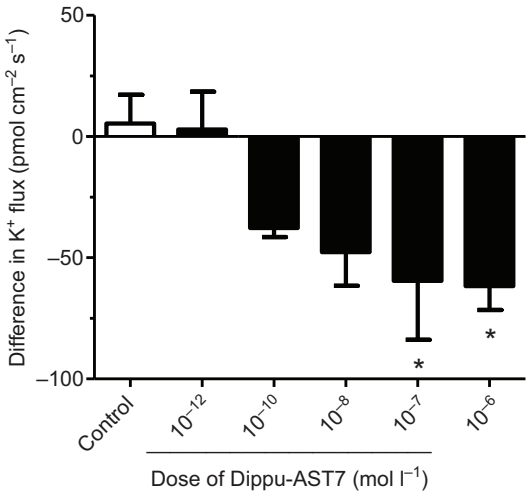

Fig. 5. Effect of Dippu-AST7 on K$^+$ absorption by the rectum of larval *C. riparius*. K$^+$ fluxes were recorded adjacent the saline-bathed rectum with the scanning ion-selective electrode technique prior to and after the addition of Dippu-AST7 at the indicated doses. Data are expressed as the difference in K$^+$ flux prior to and after addition of Dippu-AST7. Controls received addition of saline only with no peptide. Asterisks denote a significant difference from the control group (Kruskal–Wallis test, P=0.002; Dunn's multiple comparisons test, P<0.05, n=5–10).

The Journal of Experimental Biology (2014) doi:10.1242/jeb.108985

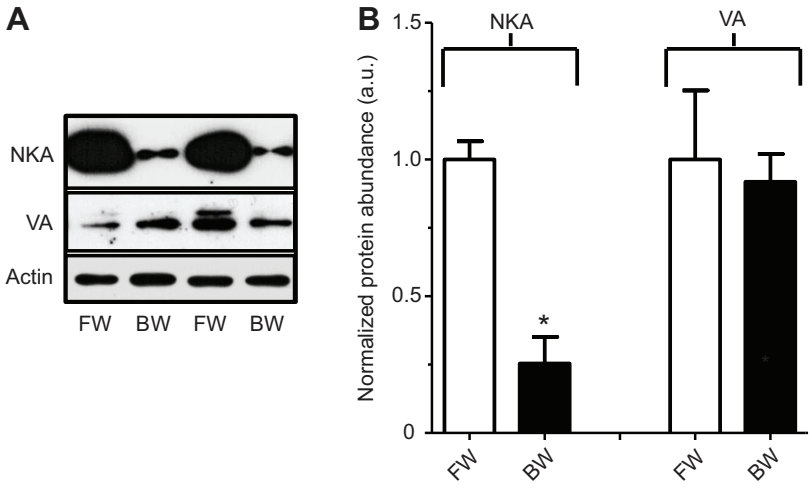

Fig. 7. NKA and VA protein expression in recta of freshwater and brackish water-reared *C. riparius* larvae. Recta were isolated from larvae reared in either freshwater (FW; control) or brackish water (BW), and then flash frozen prior to processing for Western blot analysis. (A) Representative western blot of NKA and VA protein expression in recta from FW- and BW-reared animals. (B) Densitometric analysis of NKA and VA protein abundance in recta collected from FW- and BW-reared larvae. Asterisks denote a significant difference from the FW (control) group (Student's *t*-test, $P<0.05$, $n=3$).

AST-IR endocrine cells in the midgut. The adult female mosquito contains AST-IR endocrine cells only in the posterior region of the midgut (Hernández-Martínez et al., 2005), as do larval and adult *Drosophila* (Yoon and Stay, 1995). The larval lepidopteran *C. pomonella* also has AST-IR endocrine cells confined to the posterior midgut (Duve et al., 1997), while other insects have an apparently even distribution of cells along the entire midgut (Robertson and Lange, 2010; Sarkar et al., 2003; Maestro et al., 1998). The regionalization of AST-IR endocrine cells in the midgut of dipterans and lepidopterans may be a consequence of digestive processes requiring high luminal alkalinity because these larvae have regional differences in luminal pH in the midgut (Boudko et al., 2001; Shanbhag and Tripathi, 2005; Coddington and Chamberlin, 1999). The function of the AST-IR endocrine cells in the midge is unclear. These cells may sense nutritional content and AST may affect midgut muscle, enzyme production and/or ion transport. Further study in these areas can determine the function of AST in the endocrine cells.

AST effects on hindgut muscle contraction and K^+ reabsorption

AST inhibits the contractions of the larval midge hindgut in a dose-dependent manner (Figs 3, 4). This suggests that the hindgut muscle expresses receptors for AST. Many previous studies have demonstrated that AST is a myoinhibitory peptide in insects (Sarkar et al., 2003; Lange et al., 1993; Onken et al., 2004; Duve et al., 2000). A dose of 1 pmol l^{-1} non-native AST on the foregut and hindgut of *Lacanobia oleracea* and *Rhodnius prolixus*, respectively (Sarkar et al., 2003; Duve et al., 2000), is effective at inhibiting muscle contractions. The larval midge hindgut responds to a threshold dose of 5 nmol l^{-1} non-native AST from the cockroach. This result, together with the presence of AST-IR in processes on the hindgut that originate from cells in the terminal ganglion, suggest that AST-like neuropeptides are acting as inhibitory neurotransmitters and/or neuromodulators of hindgut muscle in larval *C. riparius*. The inhibition of hindgut muscle contraction by AST should prolong the time luminal contents remain in the hindgut prior to excretion. In a previous study, our laboratory has shown that the rectum of larval *C. riparius* is a site of K^+ reabsorption and that this is dependent on the activities of NKA and VA, which are expressed on the basal and apical membranes of epithelial cells, respectively (Jonusaite et al., 2013). In that study, it was shown that the recta of larvae reared under dilute freshwater or in ion-poor conditions had relatively high NKA and VA activities and exhibited high rates of K^+ reabsorption. Conversely, the recta of larvae reared in brackish water had low NKA and VA activities and exhibited low rates of K^+ reabsorption (see Jonusaite et al., 2013). Application of AST to the larval recta decreased K^+ reabsorption in a dose-dependent manner (Fig. 5). A dose of 10 nmol l^{-1} AST also decreased the NKA and VA activities in larval recta (Fig. 6). Together, these results indicate that AST inhibits K^+ reabsorption by lowering the activities of NKA and VA in the larval recta. The actions of exogenously applied AST on hindgut motility and ion reabsorption suggest that AST functions as a general depressant of hindgut functions; however, because the rectum receives direct innervation from neurons of the terminal ganglion, it is conceivable that the modulation of muscle activity and epithelial transport can be independently controlled. Studies have shown that AST modulates gut muscle activity (Sarkar et al., 2003; Duve et al., 2000). Studies have also provided evidence that AST directly modulates ion transport activities in gut epithelia (Onken et al., 2004; Vanderveken and O'Donnell, 2014). By simultaneously and perhaps independently modulating transit time of hindgut luminal contents and the magnitude of epithelial ion reabsorption through direct neural control, the midge would greatly increase its ability to fine-tune the reabsorptive and excretory functions of the hindgut.

Modulating rectal ion reabsorption with AST and habitat salinity

The larvae of *C. riparius* are found in waters of widely varying ionic content. In dilute freshwater and ion-poor conditions, the anal papillae take up ions while the rectum reabsorbs ions, thereby countering the loss of ions and osmotic uptake of water from the dilute habitat (Nguyen and Donini, 2010; Jonusaite et al., 2013). Larvae survive abrupt transfer to, and can be reared in, brackish water (20% seawater) (Jonusaite et al., 2011; Jonusaite et al., 2013). Abrupt transfer to brackish water is accompanied by a sharp reduction in whole-body VA activity and a less pronounced decrease in whole-body NKA activity (Jonusaite et al., 2011). The greatest amount of NKA and VA activity can be attributed to the rectum, and the recta of larvae reared in brackish water have greatly reduced NKA and VA activities, which coincide with reduced ion reabsorption (Jonusaite et al., 2013).

Although the larval response to abrupt and long-term (rearing) exposure to brackish water is the same, the mechanisms with which this is achieved are likely to be different. Abrupt exposure to elevated salinity would require a rapid response that could be

The Journal of Experimental Biology (2014) doi:10.1242/jeb.108985

achieved with localized release of AST at the rectal epithelium, resulting in a rapid reduction in NKA and VA activity (Fig. 6) and subsequent rapid reduction in ion reabsorption (Fig. 5). The observed rapid response to application of AST to the rectal epithelium is likely to result from activation of AST receptors on epithelial cells and subsequent second messenger pathways that impinge on the activities of NKA and VA. This scenario would be similar to the serotonin modulation of VA activity in the blowfly salivary glands (Baumann and Walz, 2012). Larvae of *C. riparius* that inhabit regions of southern Canada and the northern United States encounter abrupt salination of their freshwater habitats in the spring when snow melt adjacent to roadways that were treated with salt in the winter enters surrounding water bodies that are inhabited by *C. riparius*. Often, these events produce substantial, acute increases in the ionic content of these bodies of water (Allert et al., 2012; Fay and Shi, 2012), and as such *C. riparius* would require a mechanism to regulate internal ion levels over the short term. Our results suggest that localized modulation of rectal reabsorption by AST could be such a mechanism.

When *C. riparius* larvae encounter sustained, long-term, elevated ionic conditions, continued synthesis and release of AST may be metabolically detrimental; therefore, reducing NKA and VA expression in the rectal epithelium would be a more feasible solution. Indeed, protein expression of the catalytic NKA α-subunit was significantly downregulated in brackish-water-reared *C. riparius* larvae when compared with freshwater-reared animals (Fig. 7). However, VA B subunit protein expression was unaltered by rearing salinity (Fig. 7). Regulation of VA enzyme activity in insect and vertebrate models has been shown to occur via many mechanisms, notably reversible dissociation of V_1 (cytoplasmic sector) and V_o (membrane sector) domains, oxidation of disulfide bonds, and translocation of VA molecules to the plasma membrane via endocytosis and exocytosis from an intracellular vesicular pool (Baumann and Walz, 2012). Our results suggest that VA activity in the rectum of *C. riparius* is regulated in such ways by AST and also by long-term exposure to elevated salinity.

Conclusions

In summary, the larvae of *C. riparius* possess neurons and midgut endocrine cells containing AST A-like factors. The extensive AST-IR processes in the brain and within the ganglia of the central nervous system (CNS) suggest that AST A-like factors may coordinate various targets to carry out important physiological roles. The presence of AST A-like factors in midgut endocrine cells suggests that one of these roles may be related to feeding and digestion. AST-IR neurons in the terminal ganglion send processes through the proctodeal nerves to directly innervate the hindgut, where AST A inhibits muscle contraction and ion reabsorption. The inhibition of ion reabsorption at the rectum is achieved by decreasing the activities of NKA and VA and could serve as an effective mechanism of ion regulation in the face of abrupt, acute increases in habitat salinity.

MATERIALS AND METHODS

Insects

A laboratory colony of *Chironomus riparius* was maintained in the Aquatic Facility in the Department of Biology at York University at 24°C under a 12 h:12 h light:dark cycle. The larvae were reared in aerated 6 l aquaria with a 2.54 cm deep layer of sand on the bottom and filled with 3 l of dechlorinated tap water. Larvae were fed every second day with TetraFin Goldfish flakes (Tetra Holding Inc., VA, USA) and the water was renewed weekly. Studies were conducted on third and fourth instar larvae.

Immunohistochemistry

The CNS and digestive system of larvae were processed to reveal AST-like immunoreactivity utilizing a rabbit polyclonal antiserum against *Diploptera puncata* allatostatin 7 (Dippu-AST7) (R-AST; kind gift from Dr Stephen Tobe, Toronto, Canada). Cross-reactivity of this antiserum to other ASTs has been previously determined (Yu et al., 1995). Larvae were pinned through the cuticle to the bottom of a Sylgard® (Dow Corning, Mississauga, ON, Canada)-lined dish filled with saline containing (in mmol l^{-1}): 5 KCl, 74 NaCl, 1 $CaCl_2$, 8.5 $MgCl_2$, 10.2 $NaHCO_3$, 8.6 HEPES, 20 glucose and 10 glutamine; pH 7.0 (BioShop, Burlington, ON, Canada). The CNS and gut were removed under saline and fixed with a solution of 2% paraformaldehyde in Millonig's buffer, at 4°C overnight or room temperature for 2 h, with the following composition (in mmol l^{-1}): 136 $NaH_2PO_4H_2O$, 120 NaOH, 67 glucose and 0.78 $CaCl_22H_2O$; pH 7.0. All subsequent incubations were performed at 4°C unless otherwise indicated. Tissues were rinsed with phosphate-buffered saline (PBS) four times at 5 min intervals and incubated in a solution containing 2% normal sheep serum (NSS), 4% Triton-X-100 in PBS for 1 h at room temperature and subsequently in a solution of 3% skim milk powder (Nestlé, North York, ON, Canada) in PBS for 24 h. The R-AST was pre-incubated at a dilution of 1:1000 in 0.4% Triton-X-100, 2% NSS in PBS for 24 h. Tissues were incubated in the 1:1000 R-AST solution for 48 h. Tissues were rinsed with PBS five times at 10 min intervals and subsequently incubated in a solution containing 1:200 affinity purified Cy3-labeled sheep anti-rabbit antibody (Sigma-Aldrich, Oakville, ON, Canada) and 10% NSS in PBS for 24 h. Tissues were rinsed with PBS 10 times over 24 h. Controls were processed in the same manner except that some were incubated in the absence of R-AST and others were incubated in a 1:1000 R-AST solution pre-absorbed with 10 µmol l^{-1} of Dippu-AST7 (APSGAQRLYGFGLamide, AnaSpec, San Jose, CA, USA). Tissues were mounted in glycerol on glass slides and viewed with a Fluoview 300 laser scanning confocal microscope (Olympus, Markham, ON, Canada) using a helium–neon (543 nm) laser, and digital images were captured with the accompanying Fluoview software package. Composite image figures were constructed using Adobe Photoshop CS2 (Adobe, Etobicoke, ON, Canada).

Hindgut motility assay

The frequency of larval hindgut contractions was monitored with an impedance monitor (UFI Model 2991, Morro Bay, CA, USA) connected to a Powerlab 4/30 and desktop computer running LabChart 6.0 software (ADInstruments, Colorado Springs, CO, USA). A semi-isolated preparation contained in a Sylgard®-lined dish and bathed in 2 ml of saline was developed. The preparation consisted of a portion of the posterior midgut with surrounding cuticle, exposed ileum and rectum, and the intact posterior section of the larva complete with anal papillae and prolegs. Minuten pins inserted into the cuticle at the base of the prolegs and the posterior midgut secured the preparation to the dish. Electrodes were fashioned from minuten pins soldered to wires connected to the impedance monitor inputs. With the aid of a stereomicroscope (Model K400 Series, Motic, Richmond, BC, Canada), the electrodes were positioned on either side of the preparation at the anterior rectum. Preparations were rinsed several times with fresh saline and then allowed to equilibrate in 1.98 ml of saline for 10 min. Contractions were monitored for the subsequent 10 min intervals prior to and after the addition of Dippu-AST7. The procedure was repeated to test several doses of Dippu-AST7 on individual preparations. Dippu-AST7 was administered by adding 20 µl of 100 times the desired dose of the peptide to the saline bathing the preparation. The addition of 20 µl of saline to the bath served as a control. The Peak Analysis feature in LabChart Pro 6.0 software was utilized to determine the number of contractions that occurred over the 10 min intervals and yield the frequency of contractions (contractions min^{-1}). Effects of individual doses of Dippu-AST7 on the frequency of contractions were determined by expressing the frequency of contractions in the presence of Dippu-AST7 as a percentage of the frequency of baseline contractions recorded during the 10 min interval prior to the addition of the peptide.

Hindgut K^+ flux measurements

K^+ concentration gradients were measured adjacent to the rectum of larval *C. riparius* with the scanning ion-selective electrode technique (SIET) and

used to calculate K^+ flux at the rectum. The hindgut preparation for these measurements was previously described in detail (Jonusaite et al., 2013). In brief, the entire gastrointestinal tract of third instar *C. riparius* was isolated in saline (see section above for composition of saline) and then positioned onto the bottom of an inverted 35 mm Petri dish lid containing 4 ml of saline. The SIET system and protocol used has been described in detail (Jonusaite et al., 2013; Rheault and O'Donnell, 2001; Donini and O'Donnell, 2005). In brief, a K^+ ion-selective microelectrode (ISME) was mounted onto an Ag/AgCl wire electrode holder (World Precision Instruments) that was connected to a headstage. The headstage was connected to an ion polarographic amplifier (IPA-2, Applicable Electronics, Forestdale, MA, USA). A 3% agar in 3 mol l^{-1} KCl bridge connected to the headstage with an Ag/AgCl half-cell (World Precision Instruments) was used as the reference electrode. The K^+ ISMEs were calibrated in solutions of 1 and 10 mmol l^{-1} KCl, resulting in a mean slope of 58.9±0.57, n=33. Measurements were taken along the length of the rectum by positioning the ISME 2–5 µm from the surface of the rectum and recording a voltage for 1 s. The ISME was then positioned 100 µm away from the original recording site, perpendicular to the tissue surface, where a second voltage was recorded for 1 s. A wait time of 4 s where no recording took place was employed after each movement of the ISME. This sampling method was then repeated four times at each site along the length of the rectum. Positioning the ISME and calculation of voltage gradients were performed using Automated Scanning Electrode Technique (ASET) software (version 2.0, Science Wares, East Falmouth, MA, USA). To account for mechanically derived disturbances in the ion gradients through movement of the ISME, control measurements were recorded using the same sampling method but at sites that were 2–3 mm away from the surface of the rectum. To calculate K^+ fluxes, the voltage gradients were first converted into concentration gradients with the following equation:

$$\Delta C = C_B \times 10^{\Delta V/S} - C_B , \quad (1)$$

where ΔC is the concentration gradient between the two points measured in µmol l^{-1} cm^{-3}, C_B is the background ion concentration, calculated as the average of the concentration at each point measured in µmol l^{-1}, ΔV is the voltage gradient obtained from ASET in µV and S is the slope of the electrode. Using the calculated concentration gradients, a corresponding flux value was then derived using Fick's law of diffusion as follows:

$$J_I = D_I(\Delta C)/\Delta x , \quad (2)$$

where J_I is the net flux of the ion in pmol cm^{-2} s^{-1}, D_I is the diffusion coefficient of the ion (1.92×10^{-5} cm^2 s^{-1} for K^+), ΔC is the concentration gradient in pmol cm^{-3} and Δx is the distance between the two points measured in cm.

Measurement of NKA and VA activities of the rectum exposed to AST

In aquaria identical to those outlined above, eggs were hatched and larvae were reared to third and fourth instar (~30 days) in ion-poor water (composition in µmol l^{-1}: $[Na^+]$ 20; $[Cl^-]$ 40; $[Ca^{2+}]$ 2; $[K^+]$ 0.4; pH 6.5). Larval recta were then isolated under saline and individually incubated with either saline (control) or saline containing 10^{-8} mol l^{-1} Dippu-AST7 for 10 min at room temperature. After incubation, the recta were collected in 1.5 ml microcentrifuge tubes (30–35 recta per tube), flash-frozen and stored at −85°C until further analysis. For NKA and VA activity assays, recta were thawed on ice and processed according to previously described methods (Jonusaite et al., 2011). NKA and VA activity assays were subsequently conducted using the methodology of McCormick (McCormick, 1993) with modifications as described by Jonusaite et al. (Jonusaite et al., 2011).

NKA and VA protein expression in recta of larvae reared in freshwater and brackish water

In the following experiment, eggs were hatched and larvae were reared as described above in brackish water composed of 7 g l^{-1} Instant Ocean Sea Salt (i.e. 20% seawater, approximately equivalent to 96 mmol l^{-1} NaCl; United Pet Group, Blacksburg, VA, USA). Freshwater (control) animals also were reared in dechlorinated tap water as described above. Recta from larvae reared in freshwater and brackish water were then isolated under saline and collected into 1.5 ml microcentrifuge tubes (25–30 recta per tube), flash-frozen and stored at −85°C until further processing. For western blot analysis, recta were thawed and homogenized on ice in chilled homogenization buffer (50 mmol l^{-1} Tris-HCl pH 7.4, 1 mmol l^{-1} phenylmethylsulfonyl fluoride) containing 1:200 protease inhibitor cocktail using glass Kontes handheld tissue grinders. Homogenates were then centrifuged at 8000 ***g*** for 10 min at 4°C, and protein content of collected supernatant was determined using the Bradford assay (Sigma-Aldrich) according to the manufacturer's guidelines. Samples were prepared for SDS-PAGE by either incubating for 10 min at 65°C for NKA samples or by boiling for 5 min at 100°C for VA samples with 5× loading buffer containing 225 mmol l^{-1} Tris-HCl (pH 6.8), 3.5% (w/v) SDS, 35% glycerol, 12.5% (v/v) β-mercaptoethanol and 0.01% (w/v) Bromophenol Blue. Equal amounts of sample (i.e. 5 µg each) were electrophoretically separated by SDS-PAGE and western blot analysis of NKA and VA was conducted according to procedures outlined by Chasiotis and Kelly (Chasiotis and Kelly, 2008) using a 1:100 dilution of mouse monoclonal anti-α5 antibody (Developmental Studies Hybridoma Bank, Iowa City, IA, USA) for NKA α-subunit and a 1:1000 dilution of rabbit polyclonal anti-ATP6V1B1 antibody (Abnova, Neihu District, Taipei City, Taiwan) for VA B subunit. After examination of NKA and VA protein expression, membranes were stripped and re-probed with a 1:100 dilution of mouse monoclonal anti-JLA20 antibody (Developmental Studies Hybridoma Bank) for actin as a loading control. Densitometric analysis of NKA, VA and actin protein was conducted using Quantity One 1D analysis software (Bio-Rad Laboratories Canada, Mississauga, ON, Canada). NKA and VA protein abundance were expressed as normalized values relative to actin abundance.

Acknowledgements

The authors thank Dr Stephen Tobe (Toronto) for providing the allatostatin antisera as a kind gift, Hang Nguyen for conducting preliminary immunohistochemical studies and Dr Marjorie Patrick (San Diego) for advising on western blot protocols for small tissues. Mouse monoclonal anti-α5 and anti-JLA20 antibodies, developed by D. M. Fambrough and J. J.-C. Lin, respectively, were obtained from the Developmental Studies Hybridoma Bank, created by the National Institute of Child Health and Human Development of the National Institutes of Health and maintained at The University of Iowa, Department of Biology, Iowa City, USA.

Competing interests

The authors declare no competing financial interests.

Author contributions

L.R., H.C. and A.D. designed the study and experiments. L.R. performed all immunohistochemistry experiments and took all resulting images. H.C. performed all experiments on AST effects on VA and NKA activities and western blots and analysed all resulting data. V.G. performed all hindgut motility assays and A.D. analysed these results. A.D. performed all experiments assessing AST effects on K^+ fluxes and analysed all resulting data. L.R., H.C. and A.D. co-wrote and co-edited the manuscript.

Funding

This work was supported by a Natural Sciences and Engineering Research Council of Canada (NSERC) Discovery Grant to A.D., and an Ontario Ministry of Research and Innovation Early Researcher Award to A.D.

References

Aguilar, R., Maestro, J. L., Vilaplana, L., Pascual, N., Piulachs, M. D. and Bellés, X. (2003). Allatostatin gene expression in brain and midgut, and activity of synthetic allatostatins on feeding-related processes in the cockroach *Blattella germanica*. *Regul. Pept.* **115**, 171-177.

Allert, A. L., Cole-Neal, C. L. and Fairchild, J. F. (2012). Toxicity of chloride under winter low-flow conditions in an urban watershed in central Missouri, USA. *Bull. Environ. Contam. Toxicol.* **89**, 296-301.

Baumann, O. and Walz, B. (2012). The blowfly salivary gland – a model system for analyzing the regulation of plasma membrane V-ATPase. *J. Insect Physiol.* **58**, 450-458.

Boudko, D. Y., Moroz, L. L., Harvey, W. R. and Linser, P. J. (2001). Alkalinization by chloride/bicarbonate pathway in larval mosquito midgut. *Proc. Natl. Acad. Sci. USA* **98**, 15354-15359.

Chasiotis, H. and Kelly, S. P. (2008). Occludin immunolocalization and protein expression in goldfish. *J. Exp. Biol.* **211**, 1524-1534.

Coddington, E. J. and Chamberlin, M. E. (1999). Acid/base transport across the midgut of the tobacco hornworm, *Manduca sexta*. *J. Insect Physiol.* **45**, 493-500.

Colbo, M. H. (1996). Chironomidae from marine coastal environments near St. John's, Newfoundland, Canada. *Hydrobiologia* **318**, 117-122.
Donini, A. and O'Donnell, M. J. (2005). Analysis of Na^+, Cl^-, K^+, H^+ and NH_4^+ concentration gradients adjacent to the surface of anal papillae of the mosquito *Aedes aegypti*: application of self-referencing ion-selective microelectrodes. *J. Exp. Biol.* **208**, 603-610.
Donly, B. C., Ding, Q., Tobe, S. S. and Bendena, W. G. (1993). Molecular cloning of the gene for the allatostatin family of neuropeptides from the cockroach *Diploptera punctata*. *Proc. Natl. Acad. Sci. USA* **90**, 8807-8811.
Duve, H., Johnsen, A. H., Maestro, J. L., Scott, A. G., Crook, N., Winstanley, D. and Thorpe, A. (1997). Identification, tissue localisation and physiological effect in vitro of a neuroendocrine peptide identical to a dipteran Leu-callatostatin in the codling moth *Cydia pomonella* (Tortricidae: Lepidoptera). *Cell Tissue Res.* **289**, 73-83.
Duve, H., Audsley, N., Weaver, R. J. and Thorpe, A. (2000). Triple co-localisation of two types of allatostatin and an allatotropin in the frontal ganglion of the lepidopteran *Lacanobia oleracea* (Noctuidae): innervation and action on the foregut. *Cell Tissue Res.* **300**, 153-163.
Faria, M. S., Ré, A., Malcato, J., Silva, P. C. L. D., Pestana, J., Agra, A. R., Nogueira, A. J. A. and Soares, A. M. (2006). Biological and functional responses of *in situ* bioassays with *Chironomus riparius* larvae to assess river water quality and contamination. *Sci. Total Environ.* **371**, 125-137.
Fay, L. and Shi, X. (2012). Environmental impacts of chemicals for snow and ice control: state of knowledge. *Water Air Soil Pollut.* **223**, 2751-2770.
Gäde, G. and Goldsworthy, G. J. (2003). Insect peptide hormones: a selective review of their physiology and potential application for pest control. *Pest Manag. Sci.* **59**, 1063-1075.
Hahn, T., Schenk, K. and Schulz, R. (2002). Environmental chemicals with known endocrine potential affect yolk protein content in the aquatic insect *Chironomus riparius*. *Environ. Pollut.* **120**, 525-528.
Hernández-Martínez, S., Li, Y., Lanz-Mendoza, H., Rodríguez, M. H. and Noriega, F. G. (2005). Immunostaining for allatotropin and allatostatin-A and -C in the mosquitoes *Aedes aegypti* and *Anopheles albimanus*. *Cell Tissue Res.* **321**, 105-113.
Johansson, O., Olsson, A. and Wieslander, L. (1986). The distribution of putative neurotransmitters in the nervous system of the dipteran *Chironomus tentans* insect larva: an immunohistochemical study using antisera to 5-hydroxytryptamine, tyrosine hydroxylase, methionine-enkephalin, proctolin and bombesin. *Neurochem. Int.* **8**, 311-326.
Jonusaite, S., Kelly, S. P. and Donini, A. (2011). The physiological response of larval *Chironomus riparius* (Meigen) to abrupt brackish water exposure. *J. Comp. Physiol. B* **181**, 343-352.
Jonusaite, S., Kelly, S. P. and Donini, A. (2013). Tissue-specific ionomotive enzyme activity and K^+ reabsorption reveal the rectum as an important ionoregulatory organ in larval *Chironomus riparius* exposed to varying salinity. *J. Exp. Biol.* **216**, 3637-3648.
Kramer, S. J., Toschi, A., Miller, C. A., Kataoka, H., Quistad, G. B., Li, J. P., Carney, R. L. and Schooley, D. A. (1991). Identification of an allatostatin from the tobacco hornworm *Manduca sexta*. *Proc. Natl. Acad. Sci. USA* **88**, 9458-9462.
Kreissl, S., Schulte, C. C., Agricola, H. J. and Rathmayer, W. (1999). A single allatostatin-immunoreactive neuron innervates skeletal muscles of several segments in the locust. *J. Comp. Neurol.* **413**, 507-519.
Lange, A. B., Chan, K. K. and Stay, B. (1993). Effect of allatostatin and proctolin on antennal pulsatile organ and hindgut muscle in the cockroach, *Diploptera punctata*. *Arch. Insect Biochem. Physiol.* **24**, 79-92.
Lee, S. B. and Choi, J. (2007). Effects of bisphenol A and ethynyl estradiol exposure on enzyme activities, growth and development in the fourth instar larvae of *Chironomus riparius* (Diptera, Chironomidae). *Ecotoxicol. Environ. Saf.* **68**, 84-90.
Li, Y., Hernandez-Martinez, S., Fernandez, F., Mayoral, J. G., Topalis, P., Priestap, H., Perez, M., Navare, A. and Noriega, F. G. (2006). Biochemical, molecular, and functional characterization of PISCF-allatostatin, a regulator of juvenile hormone biosynthesis in the mosquito *Aedes aegypti*. *J. Biol. Chem.* **281**, 34048-34055.
Maestro, J. L., Bellés, X., Piulachs, M. D., Thorpe, A. and Duve, H. (1998). Localization of allatostatin-immunoreactive material in the central nervous system, stomatogastric nervous system, and gut of the cockroach *Blattella germanica*. *Arch. Insect Biochem. Physiol.* **37**, 269-282.
Matthews, H. J., Audsley, N. and Weaver, R. J. (2008). In vitro and in vivo effects of myo-active peptides on larvae of the tomato moth *Lacanobia oleracea* and the cotton leaf worm *Spodoptera littoralis* (Lepidoptera; Noctuidae). *Arch. Insect Biochem. Physiol.* **69**, 60-69.
McCormick, S. D. (1993). Methods for nonlethal gill biopsy and measurement of Na^+, K^+-ATPase activity. *Can. J. Fish. Aquat. Sci.* **50**, 656-658.
Morales, M., Planelló, R., Martínez-Paz, P., Herrero, O., Cortés, E., Martínez-Guitarte, J. L. and Morcillo, G. (2011). Characterization of Hsp70 gene in *Chironomus riparius*: expression in response to endocrine disrupting pollutants as a marker of ecotoxicological stress. *Comp Biochem Physiol* **153C**, 150-158.
Moreau, X., Saez, G., Thiéry, A., Clot-Faybesse, O., Guiraudie-Capraz, G., Bienboire-Frosini, C., Martin, C. and De Jong, L. (2008). ELISA detection of multixenobiotic resistance transporter induction in indigenous freshwater Chironomidae larvae (Diptera): a biomarker calibration step for *in situ* monitoring of xenobiotic exposure. *Environ. Pollut.* **153**, 574-581.
Nguyen, H. and Donini, A. (2010). Larvae of the midge *Chironomus riparius* possess two distinct mechanisms for ionoregulation in response to ion-poor conditions. *Am. J. Physiol.* **299**, R762-R773.
Onken, H., Moffett, S. B. and Moffett, D. F. (2004). The anterior stomach of larval mosquitoes (*Aedes aegypti*): effects of neuropeptides on transepithelial ion transport and muscular motility. *J. Exp. Biol.* **207**, 3731-3739.
Predel, R., Rapus, J. and Eckert, M. (2001). Myoinhibitory neuropeptides in the American cockroach. *Peptides* **22**, 199-208.
Reichwald, K., Unnithan, G. C., Davis, N. T., Agricola, H. and Feyereisen, R. (1994). Expression of the allatostatin gene in endocrine cells of the cockroach midgut. *Proc. Natl. Acad. Sci. USA* **91**, 11894-11898.
Rheault, M. R. and O'Donnell, M. J. (2001). Analysis of epithelial K^+ transport in Malpighian tubules of *Drosophila melanogaster*: evidence for spatial and temporal heterogeneity. *J. Exp. Biol.* **204**, 2289-2299.
Robertson, L. and Lange, A. B. (2010). Neural substrate and allatostatin-like innervation of the gut of *Locusta migratoria*. *J. Insect Physiol.* **56**, 893-901.
Sarkar, N. R. S., Tobe, S. S. and Orchard, I. (2003). The distribution and effects of Dippu-allatostatin-like peptides in the blood-feeding bug, *Rhodnius prolixus*. *Peptides* **24**, 1553-1562.
Shanbhag, S. and Tripathi, S. (2005). Electrogenic H+ transport and pH gradients generated by a V-H+ -ATPase in the isolated perfused larval *Drosophila* midgut. *J. Membr. Biol.* **206**, 61-72.
Siju, K. P., Reifenrath, A., Scheiblich, H., Neupert, S., Predel, R., Hansson, B. S., Schachtner, J. and Ignell, R. (2014). Neuropeptides in the antennal lobe of the yellow fever mosquito, *Aedes aegypti*. *J. Comp. Neurol.* **522**, 592-608.
Skiebe, P., Biserova, N. M., Vedenina, V., Börner, J. and Pflüger, H. J. (2006). Allatostatin-like immunoreactivity in the abdomen of the locust *Schistocerca gregaria*. *Cell Tissue Res.* **325**, 163-174.
Vanderveken, M. and O'Donnell, M. J. (2014). Effects of diuretic hormone 31, drosokinin, and allatostatin A on transepithelial K^+ transport and contraction frequency in the midgut and hindgut of larval *Drosophila melanogaster*. *Arch. Insect Biochem. Physiol.* **85**, 76-93.
Veenstra, J. A. (2009). Peptidergic paracrine and endocrine cells in the midgut of the fruit fly maggot. *Cell Tissue Res.* **336**, 309-323.
Veenstra, J. A., Lau, G. W., Agricola, H. J. and Petzel, D. H. (1995). Immunohistological localization of regulatory peptides in the midgut of the female mosquito *Aedes aegypti*. *Histochem. Cell Biol.* **104**, 337-347.
Wang, J., Meyering-Vos, M. and Hoffmann, K. H. (2004). Cloning and tissue-specific localization of cricket-type allatostatins from *Gryllus bimaculatus*. *Mol. Cell. Endocrinol.* **227**, 41-51.
Williams, D. D. and Williams, N. E. (1998). Aquatic insects in an estuarine environment: densities, distribution and salinity tolerance. *Freshw. Biol.* **39**, 411-421.
Williamson, M., Lenz, C., Winther, A. M. E., Nässel, D. R. and Grimmelikhuijzen, C. J. P. (2001). Molecular cloning, genomic organization, and expression of a C-type (*Manduca sexta*-type) allatostatin preprohormone from *Drosophila melanogaster*. *Biochem. Biophys. Res. Commun.* **282**, 124-130.
Yoon, J. G. and Stay, B. (1995). Immunocytochemical localization of *Diploptera punctata* allatostatin-like peptide in *Drosophila melanogaster*. *J. Comp. Neurol.* **363**, 475-488.
Yu, C. G., Stay, B., Ding, Q., Bendena, W. G. and Tobe, S. S. (1995). Immunochemical identification and expression of allatostatins in the gut of *Diploptera puncata*. *J. Insect Physiol.* **41**, 1035-1043.
Žitňan, D., Sehnal, F. and Bryant, P. J. (1993). Neurons producing specific neuropeptides in the central nervous system of normal and pupariation-delayed *Drosophila*. *Dev. Biol.* **156**, 117-135.

The Journal of Experimental Biology